ESP PERFORMANCE UNDER TWO-PHASE FLOW CONDITIONS

Raghavan Beltur and Mauricio Prado, University of Tulsa
Javier Duran, Ecopetrol
Rui Pessoa, PDVSA

ABSTRACT
ESP performance is affected by the presence of free gas. Two-phase performance is sensitive to intake pressure, in situ gas fraction, fluid properties, speed and number of stages. The degree of head deterioration varies from the simple reduction in the pressure increment to surging and gas locking. So far, no reliable predictive method is available to predict the performance of centrifugal pumps under two-phase conditions and to address the problems of surging and gas locking. The University of Tulsa Artificial Lift Projects is currently conducting experimental and theoretical research on the two-phase behavior of centrifugal pumps. This paper presents the analysis of experimental data for two-phase flow performance of a 22-stage centrifugal pump on a stage-wise basis. The tests were conducted at 50 Hz, varying several operating conditions such as intake pressure (50 to 250 psig) and gas flow rates. Comparison of the experimental data from this work with the homogeneous model shows that the homogeneous model is not capable of correctly predicting head degradation, surging and gas locking conditions. This work is fundamental for the development and validation of models or correlations for predicting performance of ESPs under two-phase conditions.

INTRODUCTION
Centrifugal pumps are dynamic single or multistage devices that use kinetic energy to increase liquid pressure. To handle low viscosity, single-phase incompressible fluids, existing impeller and diffuser designs are very successful, but are severely impacted by free gas, highly compressible or viscous fluids.

The head performance curves provided by the manufacturers based on experimentally determined using water as the working fluid are valid then for any other low viscosity single-phase liquid, independent of its density. Brake horsepower and efficiency curves are usually presented on the same chart. The performance of multistage pumps handling incompressible fluids is presented on average per stage. An example of these performance curves is shown in **Figure 1**.For low viscosity oil with no free gas or very low volumetric free gas fractions (< 2%) at pump intake condition, the sizing of a multi-stage ESP has shown good agreement based on the water performance curves supplied by the manufacturer, corrected by the homogeneous model approach.

While handling higher contents of free gas, the centrifugal pump suffers head degradation. Performance prediction based on single-phase water Performance curves corrected by the homogeneous model cannot be used. In addition to performance degradation while handling free gas, submersible pumps also require prediction of surging and gas lock conditions. The homogeneous model is incapable of correctly addressing these problems.

Surging is a phenomenon related to instability of the pump performance. Studies from the nuclear industry state that surging appears as a discontinuity in the head performance, and such discontinuity is a consequence of a change in flow pattern from dispersed bubble or turbulent churned flow to stratified or slug flow. This abrupt fluctuation in performance is observed for flow rates smaller than the best efficiency point and changes with the amount of gas at the pump intake. An example of the pressure fluctuation during surging, with respect to time, is shown in **Figure 2.**

Gas lock is the next deteriorating stage after surging. During gas lock conditions, the pump stops delivering head. Once the pump is locked, it could be brought to normal operating condition by either increasing the intake pressure or stopping the pump so that gas is pushed out of suction by liquid.

A comparison between the experimentally determined head performance for the pump used in this study and the predicted performance, using the homogeneous model, is shown in **Figure 3.** One can see that the actual two-phase flow performance is considerably different from the single-phase performance and from the homogenous model. In order to correctly design, analyze and troubleshoot ESP applications in gassy environments, the performance of ESP under multiphase conditions must be known. Additionally, extensive theoretical and experimental research must be conducted to better understand this complex phenomenon.

LITERATURE REVIEW:

Few studies are available in the literature regarding the behavior of centrifugal pumps handling two-phase mixtures. The petroleum industry is mainly concerned with multi-stage small diameter pumps (electric submersible pumps) while the nuclear industry focuses on single-stage, higher diameter pumps.

Most of the petroleum industry research has been of an empirical nature, which is perfectly understandable, due to the complexity of the phenomena that rule centrifugal pump behavior. The isolated experiments conducted so far have been fundamental to understand tendencies and to provide insight on real behavior of ESP's when handling multiphase flow.

Before reviewing previous works, it is necessary to understand how the industry presently designs the pumps for gassy applications based on the homogeneous model.

HOMOGENEOUS METHOD FOR ESP MULTIPHASE PERFORMANCE:

In the homogeneous model, the mixture is considered homogeneous. The no-slip mixture flow rate is the sum of the liquid and the gas flow rates at pump (or stage) intake conditions. The two-phase head is calculated based on the single-phase water head curve provided by the manufacturer at this total mixture flow rate. The two-phase head, or the mixture head, $H_{stage}^{tp}\{q_l, q_g\}$, as a function of gas and liquid flow rates is then given by:

$$H_{stage}^{tp}\{q_l, q_g\} = H_{stage}^{sp}\{q_m\}, \qquad (1)$$

where q_l and q_g are the in-situ liquid and gas flow rates, respectively and $H_{stage}^{sp}\{q_m\}$ is the stage single-phase head from the manufacturer water based curves at the total mixture flow rate.

The mixture flow rate q_m is expressed as sum of in-situ liquid and gas flow rates:

$$4, = 4 /\!+ q_g . \qquad (2)$$

The stage two-phase head can be related to the stage two-phase pressure increment based on the no-slip mixture density $\rho_m^{no\ slip}$ at average stage inlet pressure and temperature conditions. The stage two-phase pressure increment, ΔP_{singe}^{tp}, is given by:

$$\Delta P_{stage}^{tp} = H_{stage}^{tp} \ \rho_m^{no\ slip} \ g, \qquad (3)$$

where the no-slip mixture density $\rho_m^{no\ slip}$ is a function of the in-situ flow rates and no-slip gas void fraction λ_g and is expressed as:

$$\rho_m^{no\ slip} = (1 - \lambda_g)\rho_l + \lambda_g \rho_g, \qquad (5)$$

The homogeneous model given by Eq.1 can be expressed then as:

$$H_{stage}^{tp}\{q_l, \lambda_g\} = H_{stage}^{sp}\{\frac{q_l}{1 - \lambda_g}\} \qquad (6)$$

The two-phase head prediction based on single-phase head, provided by the manufacturer, using Eq.6 is demonstrated in **Figure 4.** An example of the two-phase head based on single-phase head for different gas void fractions for a specific pump is shown in **Figure 5.**

A common practice in the industry is to compare the stage two-phase flow head with the manufacturer's single-phase water head based on the same density reference. If the water density ρ_w is used as a reference for the stage two-phase flow head, the following equation can be written:

$$\Delta P_{stage}^{tp} = h_{stage}^{tp}\, g\, \rho_w, \tag{7}$$

where h_{stage}^{tp} is the two-phase head based on the water density. The lower case *"h"* is used to make clear distinction with "*H*" which is based on mixture density.

The relationship between the two definitions of stage two-phase flow head can be obtained by combining Eq. 3 and 11.

$$H_{stage}^{tp}\, \rho_m^{no\ slip} = h_{stage}^{tp}\, \rho_w. \tag{8}$$

The water based two-phase flow head h_{stage}^{tp} can also be written as:

$$h_{stage}^{tp}\{q_l, \lambda_g\} = \left[(1-\lambda_g) + \frac{\lambda_g \rho_g}{\rho_w}\right] H_{stage}^{sp}\{\frac{q_l}{1-\lambda_g}\}. \tag{9}$$

The two-phase water head prediction, based on the single-phase head provided by the manufacturer using Eq.9, is demonstrated in **Figure 6.** An example of the two-phase head based on single-phase head for different gas void fractions for a specific pump is shown in **Figure 7.**

It appears from **Figure 7** that head degradation is accounted for in the homogeneous model. In reality, what **Figure 7** shows is degradation in pressure due to the reduction in mixture density. It is very important to highlight that in the homogeneous model, no head degradation is accounted for, as indicated by Eq. 1.
The head predictions based on the homogeneous model provides a good approximation when the mixture is truly homogeneous inside the pump. Homogeneous flow can occur only at low gas void fractions.

A comparison of two-phase experimental results against the homogeneous model prediction is shown in **Figure 8** for 10th stage at constant gas mass rate of 30000 SCFD and at pumps intake pressure of 100 psig. This figure shows the considerable performance degradation in entire range of liquid flow rate and higher degradation exists for higher gas void fractions, which are not captured by the homogeneous model. In addition, the homogeneous model predicts the peak performance where the surging in general is more predominant. It can be seen that the homogeneous model fails to correctly predict surging conditions.

Note: The word "Peak Performance'' should not be confused with best efficiency point. Where ever the peak "Peak Performance'' is mentioned, it refers to the point at which highest-pressure increment is developed.

Application of the homogeneous model should then be limited to low gas void fraction where the mixture can be considered truly homogeneous. Consequently, one should be interested in determining what the intake conditions are and where the homogeneous model will correctly predict two-phase flow performance. This was the main objective of Dunbar (1989) work presented next.

Dunbar (1989) presented a procedure to determine the proper pump intake conditions, where the homogeneous model could be applied successfully.

The author used the "vapor liquid ratio" (*VLR*), which is the ratio of the in-situ volume of free gas to the in-situ volume of liquid, as an independent variable. The author coins this term to avoid confusion with surface or producing gas liquid ratio.

$$VLR = \frac{q_g}{q_l}, \tag{10}$$

where q_g and q_l are in-situ gas and liquid flow rates

Using field data, Dunbar constructed a reference curve called, the "Dunbar Curve", shown in **Figure 9.** This shows a plot a for the minimum intake pressure that should be attained for a given gas liquid ratio, to apply the homogeneous model or to account for no head degradation.

The region above the Dunbar curve in **Figure 9,** referred to as *"OKforpumping"* originally by the author, is the region where the homogeneous model can be applied. In this region, the minimum intake pressure condition for a specific vapor liquid ratio is satisfied. The region below the Dunbar curve, referred to, as *"notOK for pumping"* originally by the author, is the region where the homogeneous model fails to predict two-phase head performance. For the operating conditions below the Dunbar curve head degradation should be accounted for. To account for head degradation, Dunbar defines two auxiliary factors, VLR_{ALIM} and VLR_{BLIM} as shown in **Figure 10.** VLR_{ALIM} is the value of the vapor-liquid ratio on the Dunbar curve for the operating intake pressure where no head degradation is expected. VLR_{BLIM} is the value of the maximum vapor-liquid ratio for the operating intake pressure where the pump generates no head. This point can also be referred to as gas locking. Unfortunately, the author does not provide any correlation or criteria to determine the value of VLR_{BLIM} and advises to rely on the experimental data or experience when determining this value. The head degradation below the Dunbar curve is given as a linear function from VLR_{ALIM} to VLR

The best curve fit equation for Dunbar's *ALIM* curve obtained in this work is given by:

$$P_i^{\min} = 935\,(VLR)^{1/1.724} \qquad (11)$$

where $P_i^{\min}$ is the minimum intake pressure that should be attained for a given *FGLR* to apply the homogeneous model.

The graph shown in **Figure 10** presents the Dunbar curve superimposed with two *"GasIngestion Percentage or GIP curve"*. The *"Gas Ingestion Percentage or GIP Curve"*, is the value of *VLR* that exist at the pump intake for a certain application. This curve is a function of PVT data, production data, separation efficiency, reservoir performance and pressure drop between the perforations and the pump intake location. Gas ingestion percentage is the percentage of total gas at in-situ condition entering the pump. The curve of 100% *GIP* shown in **Figure 10** represents the vapor liquid ratio, with respect to intake pressure, when 100% of in-situ gas is entering the pump. With 90% efficiency of gas separation, only 10% of in-situ gas will enter the pump and the *VLR* curve follows the 10% *GIP* curve. The *GIP* curves shown in **Figure 10,** are calculated based on Standing correlation for *PVT* data for an oil of API-21, gas specific gravity of 0.7, bottom hole temperature of 200^{0}F, *GOR* of 350 SCF/STB and water cut of 50%. For the data plotted, the bubble point pressure is 2600 psig.

According to Dunbar, the homogeneous model can be applied for the operating conditions in the region above the Dunbar curve, VLR Here in this region, no head degradation is expected. For the operating condition below the $VLR_{ALIM,}$ head degradation should be accounted as explained earlier. Below the VLR_{BLIM}, no head is generated and requires a suitable gas separator to modify the intake condition so that operating condition falls at least above the VLR_{BLIM} curve. Using a gas separator for operating conditions above the Dunbar curve will help in increasing mixture density, and in turn, the stages will generate higher-pressure increment. The effect of separators on the performance of ESP depends upon where the operating conditions fall after gas separation. In the region between VLR_{ALIM} and VLR the effect of gas separators will reduce the head degradation.

A comparison was made to verify the Dunbar's criteria of minimum intake pressure required for no head degradation against Cirilo's (1989) experimental data. The plots for two-phase head based on the homogeneous model and experimental data points for 10, 15 and 20% gas void fraction are shown in **Figures 11, 12 and 13** respectively. Table 1 shows the *VLR* and minimum intake pressure, $P_i^{\min}$ **,** that is required, based on Dunbar curve for each.

Table 1
Minimum Pressure Required Based on Dunbar (1989) Curve

Gas Void Fraction	*VLR*	$P_i^{\min}$ (Psig)
10%	0.1111	261

15%	0.176	341
20%	0.25	418

It can be seen from Table 1, that for a *VLR* of 0.111 minimum pressures required to avoid head degradation is 261psi from Dunbar curve. At intake pressures of 300,400 and 500 psig, the experimental data are close to the homogeneous model predictions, as shown in **Figure 11.** Whereas, for *VLR* of 0.176 and 0.25, experimental results show a considerable difference in two-phase head at pressures exceeding the minimum pressure that should be attained for applying the homogeneous model, as shown in **Figure 12 and 13.** This comparison shows the validity of the homogeneous model at a low *VLR*, but shows considerable head degradation at higher *VLR*. Also these results show that the validity of application of Dunbar approach needs further investigation.

An important contribution of Dunbar's approach is the general criteria for the application of the homogeneous model for head prediction in two-phase flow. But the validity of this approach for different types of pump must be investigated. Moreover, no criteria or model is given to predict *BLIM.* In addition, no surging conditions are taken into consideration.

Lea and Bearden (1982) conducted experiments on 1-42B, C-72 radial flow type pumps and K-70 mixed flow type using air-water and diesel-C02 as test fluids. Experiments were conducted to map the pump performance, varying intake pressure and gas void fraction. The authors also compared the performance of axial flow type pumps with mixed flow type pumps.

This study provided the following conclusions:

- For a constant gas fraction at the pump intake, head degradation decreases as the intake pressure increases.
- The flow conditions become unstable when the gas at the pump intake exceeds certain critical limits. For the air-water tests, the critical limit was approximately 10% gas by volume at 25 psig of intake pressure. For the diesel-C02 tests, the critical limit was found to be about 15% at 50 psig.
- Pump performance also depends on the stage geometry and hydraulic design. The mixed flow impeller style pumps handle gaseous fluids better than the radial stage style pumps. Also, for similar intake pressures and gas fractions, pump operation was found to be more stable when operating to the right of the best efficiency point (BEP).

Turpin (1986), using the data of Lea and Bearden, developed empirical correlations to predict the head-capacity curve for the studied pumps as a function of the free gas-liquid ratio and pump intake pressure. Establishing a functional form for these equations required considerable trial and error. The controlling factors used to describe the deterioration of head were the free gas-liquid ratio, the pump intake pressure and the intake liquid flow rate. Cross-plots indicated a general exponential decay in performance as a function of free gas fraction. The resulting correlation for the I-42B and K-70 pumps is achieved by

$$\frac{H_{tp}}{H_{sp}} = e^{-a_1(q_g / q_l)} \tag{12}$$

where H_{tp} is the two-phase flow head (ft), H_{sp} is the single phase head (ft) from the manufacturer's curve with respect to liquid flow rate (q_l), 4, and (q_l) are the volumetric flow rates of gas (bbl/d) and liquid (bbl/d), respectively, at pump intake conditions, and a, is a parameter given by,

$$a_1 = \frac{346430}{P_i^2}\left(\frac{q_g}{q_l}\right) - \frac{410}{P_i} \tag{13}$$

where P_i is the pump intake pressure in psia.

For the C-72 pump, similar correlations are given by,

$$\frac{H_{tp}}{H_{sp}} = e^{-a_2(q_g/q_l)}[1-0.0258(q_l-b)+0.00275(q_l-b)^2-0.0001(q_l-b)^3] \tag{14}$$

where a_2 and Q_D are given, respectively, by,

$$a_2 = \frac{285340}{P_i^2}\left(\frac{q_g}{q_l}\right) \tag{15}$$

$$b = 98.3 - 33.34 \tag{16}$$

The parameter ϕ is calculated through the following equation,

$$\phi = 2000\left(\frac{q_g/q_l}{3P_i}\right) \tag{17}$$

An unexpected result is that pumps 1-42 and K-70 share the same correlation, although they are of different hydraulic design. The I-42B stage is of radial type, while the K-70 is a mixed flow type.

To check the region of unacceptable pump performance, Equation 17 can be used as criterion. These correlations are fairly accurate and valid only to the right of best efficiency point and for value ϕ less than or equal to 1. When ϕ is greater than 1, the pump is susceptible to significant head degradation and the author also specifies that performance in this region, in general, is so poor that the operation in this region should be avoided. The head correlations given by Eqations 12-14 can be used to estimate the expected head.These correlations are pump specific and can predict the head capacity curve fairly well for low gas volumes at low intake pressures and for higher gas volumes at higher suction pressures. The prediction falls off in the direction of higher gas and lower pressure conditions; however, the region of poor predictive capability of these correlations coincides with the region of unacceptable pump performance.

Sachdeva (1989) presented the first comprehensive model developed in the petroleum industry. His work was an adaptation of the nuclear industry models to the multistage pumps used on ESP.

This work was not experimental in nature, but is included in the review since data from Lea and Bearden (1982) was used to calibrate the model and to develop a correlation for the two-phase flow head.

Cirilo (1998) conducted experimental studies with three different pumps of 540 series using air-water as test fluid. The pump GN 2000 was of radial type with 35 stages and pumps GN4000 and GN7000 were of mixed type, having 18 and 13 stages, respectively. Reported the mixture head at the average pressure and temperature condition of the pump against liquid flow rate for different intake conditions.

Experiments were carried out at different intake pressure up to 450 psig with varying gas fractions at the inlet. The effects of pump rotational speed were studied with GN4000 at 45, 55 and 65 HZ, corresponding to 2650,3250 and 3850 rpm. To study the effect on average performance of the pump with number of stages, the pump GN4000 was tested with 18, 12 and 6 stages.

The performances of mixed type pumps GN7000 and GN4000 at different intake conditions conclude that the two-phase head performance deteriorates with increase in amount of gas at the intake for a constant intake pressure. The range of liquid flow rate for stable operation also reduces.

Cirilo gives a simple correlation for maximum in situ gas void fraction, $\lambda_g^{\max}$, that the pump can tolerate at given intake pressure P_i before the pump gets gas locked and mentions the correlation is valid for gas void fraction greater than 15% and does not depend on pump speed or the number of pump stages.

$$\lambda_g^{max} = 0.187 P_i^{\ 0\ 4342} \tag{18}$$

The effect on the two-phase head performance with the increase in intake pressure for constant gas void fraction was studied with the GN 7000. As expected, the head performance improved with increase in intake pressure, up to a certain pressure. Beyond a certain critical intake pressure, no improvement was seen in the two-phase head performance. For 10.5% gas fraction, performance beyond 200 psig is the same, and similarly for 15% gas performance remains same beyond 400 psig.

The effect of rotational speeds on two-phase performance for the pump GN4000 with 18 stages was studied at 45, 55 and 65 HZ. The author reported little difference in the pump's performance and stability with change in speed.

Comparing the performance of GN7000, which is highly axial, with the GN4000, the author states that the GN7000 pump exhibits less head deterioration than the GN4000.

The effect on the average performance of the pump with number of stages was studied. For higher gas void fractions, there is marked improvement in average performance with the increase in number of stages, as downstream stages handle fewer amounts of gas and higher density mixture.

Cirilo concludes that the gas handling capacity of a radial pump is much less than that of mixed type pumps. At 500-psig intake pressure, radial pumps can handle only 18% gas. Beyond 18% void fraction, the pump gets gas locked and delivers no head. Whereas, mixed type pumps deliver stable head performance, up to 27% gas void fraction at 500-psig intake pressure.

Romero (1999) conducted experiments with the Advance Gas Handler (AGH) with 12 stages in downstream and 12 stages GN4000 pump in upstream. The outlet of AGH was directly connected to the inlet of the GN4000 pump. Only pressure and temperature were measured between AGH and GN4000. To compare the AGH with GN4000, Romero has taken Cirilo's experimental data.

First, Romero developed an empirical correlation for dimensionless two-phase head developed by the GN4000 pump based on Cirilo's experimental data.

These correlations are given by the following expressions,

$$H_{tp}^{d} = (1 - q^{*})\left(a\left(q^{*}\right)^{2} + q^{*} + 1\right) \tag{19}$$

q^* is a correlation factor calculated based on factor b and dimensionless liquid flow rate, q_l^d, and is given by:

$$q^{*} = \frac{1}{b} q_l^d \tag{20}$$

Finally, a and b are the correlation factors based on free gas volumetric fraction λ_g,

$$a = 2.902\lambda_g + 0.2751, \tag{20}$$

$$b = 1 - 2.0235\,a, \tag{21}$$

Another correlation was developed to determine the minimum limit for the liquid flow rate for stable performance. Surging was observed for the liquid flow rates smaller than the minimum liquid flow rate. In a dimensionless form, as a function of gas void fraction, it is given as:

$$q_l^d \Big|_{surging} = -6.6465\lambda_g^{\ 2} + 3.5775\lambda_g + 5.4 * 10^{-3} \tag{21}$$

The author also provides a two-phase head correlation for tested AGH and is given as:

$$H_{tp} = H_{sp}^{shut\,in}\left(1-\frac{q_l}{q_{\max}^l}\right) \tag{22}$$

wher e $H_{sp}^{shirt\,in}-$ 49.03 ft/stage, taken from experimental data.

The correlation for maximum liquid flow rate $q_{\max}^l$ as a function of gas fraction is given as:

$$q_{\max}^l = 6345 - 410^7 \lambda_g{}^{5.1068} \quad For \quad \lambda_g < 0.15 \tag{23}$$

and

$$q_{\max}^l = -9144.9\lambda_g + 5515.2 \quad For \quad \lambda_g > 0.15 \tag{24}$$

A dimensionless correlation for minimum liquid flow rate required to avoid surging is given by:

$$q_l^d\Big|_{surging} = -37552\lambda_g{}^2 + 21086\lambda_g + 75.419 \tag{25}$$

Romero provides a correlation for head performance for both the GN4000 pump and AGH. Experimental studies on the AGH provide good insight on better gas handling capacity of AGH compared to a conventional pump. However, application of AGH alone, or in combination, is still not well defined. The reference single-phase curve is still not available from the manufacturer for AGH and needs more study for two-phase behavior.

Pessoa (2000): It has been seen that all the authors mentioned in this literature review have taken mixture density at the average condition of the pump and liquid flow rate at the intake of the pump. The head calculation, based on average pressure condition, is not appropriate, as volume and density of two-phase mixture varies continuously all along the pump. This results in continuous changes in density and flow rate from intake to output. The average condition for the pump varies with the number of stages, and reporting results on average condition for each stage results in discrepancy. For the first time, Pessoa collected pressure increment data across each stage and measured flow rate as mass flow rate through mass flow meters. Though no correlation was developed, stage-wise experimental data will be of great use for future works. For the first time, the author presents the results on two-phase efficiency; based on the average BHP and the average pump hydraulic horsepower.

While studying stage-wise behavior, it was observed that each stage behaves differently. The author concludes this is due to geometric differences in each stage. Experiments were conducted, keeping gas flow rate constant and varying only liquid flow rate at a constant intake pressure of 100 psig.

Beltur (2002): Continued and extended the experimental work initiated by Pessoa, conducting several tests at different gas rates at 50 **Hz** (RPM 2916) and at the intake pressures of 50, 100, 150, 200 and 250 psig.

Beltur analyzed the data acquired by Pessoa (2000) and his own data, and a detailed analysis will be shown in the following section.

EXPERIMENTAL RESEARCH AT TUALP

In 2000, Pessoa used a GC 6100, 22-stage pump, modified to measure the pressure after each individual stage. The pump with gauges fitted on stages is shown in **Figure 14.** Temperature transmitters were used to measure temperatures only at the inlet and the discharge points and the liquid and gas flow rate were measured using mass flow meters.

Selecting air-water as the test fluid has certain advantages. The solubility of air with water is negligible. With the familiar knowledge of the physical properties of both fluids, it is possible to determine exact physical properties across each stage. This will help in determining the performance of each stage. With air-water as the testing fluid, the pump faces the worst condition in two-phase flow, as the separation of air with water is very fast, compared to oil and gas. Other advantages are that it costs less; it is safe and environmental friendly. A layout of the facilities setup is shown in **Figure 15.**

SINGLE PHASE TESTS

The single-phase tests were conducted to compare the performance with the manufacturer-supplied curve. These tests were conducted at 50 Hz at intake pressures 100, 150, 200 and 250 psig to check the repeatability of single-phase performance. Reasonable repeatability was observed. An example showing the stage-wise pressure increment for single-phase at the pump intake pressure of 100-psi is shown in **Figure 16.** From **Figure 16,** it can be seen that each stage performance is different and just considering one average pump performance for analysis will not be a good approach. For comparison, stage-wise performance fits were generated. Based on data collected at four different intake pressures, trend line curves were defined for single-phase stage-wise performance. As an example, single-phase performance of the 10th stage with the polynomial fit is shown in **Figure 17.**

As each stage performance is different on actual flow rates, a new approach based on dimensionless flow rates and dimensionless pressure increments was considered.

The dimensionless pressure increment is expressed as a ratio of pressure increment to shut in pressure increment. Shut in pressure increment is the pressure increment recoded at zero liquid flow rate.

$$\Delta P^{d}_{n\,Stage} = \frac{\Delta P_{n\,stage}}{\Delta P^{SP}_{n\,Stage\,shutin}} \tag{26}$$

Similarly, the dimensionless flow rate is expressed as:

$$q^{d}_{l_{n\,Stage}} = \frac{q_l}{q^{SP\max}_{l_{n\,Stage}}} \tag{27}$$

where $q^{SP\max}_{l_{n\,Stage}}$ is the maximurn liquid flow rate for the stage at which the pressure increment is zero.

Both the maximum single-phase liquid flow rate and shut in pressure increment were calculated based on performance polynomial fits of the stages. It can be seen from **Figure 18** that, except for the first stage, all other stages fall more or less in the same narrow range.

ANALYSIS OF TWO-PHASE DATA

Two-phase data were collected, keeping pump speed constant at 2916 RPM (50 HZ) at intake pressure from 50 psig to 250 Psig in steps of 50 Psig increment. For a set of data, maintaining constant pump intake pressure and gas flow rate, only liquid flow rate was varied from maximum flow rate to minimum possible or zero liquid flow rate. Total number of data points collected was 1944.

STAGE-WISE TWO-PHASE PERFORMANCE

An example of stage-wise performance for a gas rate of 30000 scfd at different intake pressure is shown in **Figure 19.** Stage-wise two-phase pressure increment performance shows that each stage has a different performance. Performance of the initial stages is very poor compared to the performance of downstream stages. The result of 100-psig-intake pressure shows very poor performance in the first two stages, as the mixture flow is not homogeneous and the stage intake gas fraction is high. As the mixture moves progressively to the downstream stages, the mixture gets more homogeneous due to turbulence generated by the speed of the impeller, and the gas fraction reduces due to increment in pressure in each stage. This promotes better intake conditions towards downstream stages. Due to better intake conditions, the downstream stage provides better performance.

From **Figure 19,** it can also be observed that with the increase in the intake pressure, the liquid flow rate, at which maximum pressure increment is developed, moves towards a lower flow rate. I.e. with the increase in pump intake pressure, the operable range of liquid flow rate increases.

As the liquid flow rate reduces, the pressure increment increases to a certain value of liquid flow rate, at which stage shows peak performance. To the left of this peak performance liquid flow rate, the two-phase performance of the stages drops with a steep positive slope. This sudden drop in performance can be attributed to a change in the flow regime from bubbly flow to slug flow. As the liquid flow rate is reduced further, recovery in pump performance is observed. This recovery may be due to the homogeneous nature of a mixture with higher mixture density than gas, as the flow regime may be in annular or mist flow.

As seen earlier, the dimensionless single-phase performance for all stages falls in a narrow range. An example of dimensionless plot of two-phase flow is shown in **Figure 20** for a gas flow rate of 30000 scfd and at different intake pressure.

It can be seen in dimensionless plots the two-phase performance falls on same trend only to right of peak performance liquid flow rate.

PRESSURE DEGRADATION

In order to check for the trend in degradation of pressure with respect to the single-phase and homogeneous model, data of pressure degradation were plotted against dimensionless liquid flow rate and liquid flow rate.

Pressure degradation, with respect to single-phase D_P^{SP} , is the difference between the pressure increments for the considered liquid flow, based on the single–phase performance trend line and actual pressure increment in two-phase flow condition at the same liquid flow rate.

$$\boldsymbol{D_P^{SP} = \Delta P_{SP} - \Delta P_{TP}} \tag{28}$$

Similarly, pressure degradation on the homogeneous model, $\boldsymbol{D_P^{HOM}}$ **,** is the difference between the homogeneous pressure increments at total mixture flow rate on single–phase performance trend line and actual pressure increment in two-phase flow condition at the same liquid flow rate.

$$\boldsymbol{D_P^{HOM} = \Delta P_{HOM} - \Delta P_{TP}} \tag{29}$$

The plot of degradation on a stage-wise basis, with respect to single-phase and homogeneous is shown in **Figures 21 and 22,** respectively. The stage position has an important effect on degradation. From **Figure 21,** it can be seen that the downstream stages show less degradation compared to the upstream stages.

While comparing stage degradation with the homogeneous model shown in **Figure 22,** it can be seen that downstream stages at certain liquid flow rates show very small degradation. Degradation with respect to the homogeneous model is observed to the left and right of this flow rate. This shows that the homogeneous model can be applied only after a certain number of stages, and works only at a certain liquid flow rate.

An example of the effect of stage position is shown in **Figure 23** for the test conducted at 50 psig. The plot shows that downstream stages perform much better and the range of liquid flow rate where the pump can be operated successfully increases with the number of stages.

The performance of the pump and the effect of intake pressure are of paramount importance. The amount of gas handled by the pump increases with the intake pressure. Comparing the results at 50 psig, shown **in Figure 23,** with the results at 200 psig intake pressure, shown in **Figure 24,** at 50 psig intake pressure, the pump almost stops performing beyond 12500 SCFD, while at 200 psig intake pressure, similar conditions were observed at around 65000 SCFD of gas flow rate.

The effect of pump intake pressure was studied and an example for the 16th stage at different gas flow rates is shown in **Figure 25.** It can be seen again here that for a considered gas flow rate with the increase in intake pressure, stage performance improves and peak performance liquid flow rate moves to a lower liquid flow rate. It is interesting to note that at certain liquid flow rates, the two-phase performance is almost the same at different pressures. This effect was seen in degradation plots shown earlier.

Average Pump Efficiency and Average Brake Horse Power (BHP) comparisons were made to observe the behavior of these two parameters. Stage-wise efficiency could not be calculated, as it is difficult to know the BHP consumed by each stage, because it is known that each stage performance is different and intake condition and volumetric flow rate is different. Stage-wise hydraulic horsepower is calculated considering both isothermal and adiabatic compression of gas.

The raw data records the RFM and torque in pounds-inches. The BHP consumed by an average stage is calculated by:

$$\text{BHP} = rpm(\tau\ 163025.36) \tag{30}$$

The efficiency η of the average pump is given as:

$$\eta = \frac{Hy.HP_{Liquid} + Hy.HP_{Gas}}{BHP} \tag{31}$$

Where $Hy.HP_{Liquid}$ and $Hy.HP_{gas}$ are the hydraulic horsepower for liquid and gas delivered by the pump.

Liquid hydraulic horsepower $Hy.H.P_L$ is given by:

$$Hy.H.P_L = \Delta P * \frac{144}{60*550} * \frac{q_l * 5.614587}{24*60} \tag{32}$$

Where ΔP is the pressure increment in psig and q_l is the liquid flow rate in BPD.

As the gas compression process is not clearly understood inside the stages, the gas hydraulic horsepower was calculated considering both the adiabatic and isothermal process. On a stage-wise calculation, a very small difference was found, as pressure and temperature increment on each stage is small.

Gas hydraulic horsepower adiabatic $Hy.H.P_{g\ adiabatic}$ is given by:

$$Hy.H.P_{g\ adiabatic} = \frac{144}{60*550} * \frac{M_g}{24*60} * \frac{10.7316*(T+460)}{28.9700} * \left(\left(\frac{P_2}{P_1}\right)^{\left(\frac{K-1}{K}\right)} - 1\right) * \frac{K}{K-1} \tag{33}$$

Gas hydraulic horsepower isothermal $Hy.H.P_{g\ isothermal}$ is given by:

$$Hy.H.P_{g\ isothermal} = \frac{144}{60*550} * \frac{M_g}{24*60} * \frac{10.7316*(T+460)}{28.9700} * LN\left(\frac{P_2}{P_1}\right) \tag{34}$$

Where M_g is gas mass flow rate in pounds per day, k is equal to 1.400, T is temperature at the intake of the stage in degrees F, P_2 and P_1 are pressures at discharge and intake of the stages, respectively in psig.

A plot for comparison of average two-phase BHP consumption with respect to single-phase is shown in **Figure 26.** Here again, it can be observed with increase in gas flow rate that the BHP consumption decreases.

A plot for efficiency based on adiabatic horsepower is shown in **Figure 27.** It can be seen here that with the increase in gas rate, the best efficiency point moves towards higher liquid flow rate.

CONCLUSIONS

1. The petroleum industry lacks a general model to predict an ESP's performance under two-phase flow conditions.
2. Available correlations for predicting pump performance under two-phase flow conditions are limited and are based on average pump performance. Previous correlations are pump specific and limited to the number of stages used in

the test setup.

3. The hydrodynamic conditions vary across each stage over the pump. This results in a variation in pump performance and also in horsepower consumption. Any prediction based on average performance may lead to erroneous results.
4. Dunbar (1989) developed a correlation for predicting the conditions where pump performance could be obtained using the homogeneous model. He also presented a procedure to account for head degradation when the homogeneous model cannot be applied. Critical parameters for application of this procedure were not presented.
5. From the experimental results of Cirilo (1998), it can be seen that for a constant gas fraction, the pump performance increases with increase in intake pressure until a critical pressure beyond which any increase in intake pressure will not result in improvement in pump performance. This can be compared with the region above the *ALIM* curve of Dunbar (1989).
6. Romero (1999) developed correlations for head performance and minimum liquid flow rate at which surging occurs as a function of gas void fraction. The applicability of the correlation was found to be limited to the pump with a specific number of stages and intake pressure was not considered.
7. The current TUALP research program has concluded single- and two-phase water-air stage-wise performance data for a 22-stage pump at an intake pressure of 100 psig at 55 Hz, and intake pressures of 100, 150, 200 and 250 psig at 50 Hz.
8. The average behavior of the pump is significantly different from the one observed for each stage.
9. The average best efficiency point in terms of liquid flow rate increases as gas flow rate increases.
10. The behavior of the pressure increment and total hydraulic horsepower is different for each of the stages.
11. Current knowledge is not sufficient to develop a general and accurate model for predicting head degradation, gas lock and surging conditions.
12. The performance data obtained in this work is limited to air-water mixtures.

REFERENCES

1. Cirilo, R.: *Air- WaterFlow ThroughElectric Submersible Pumps,* MS Thesis, The University of Tulsa, Oklahoma (1998).
2. Lea, J.F. and Bearden, J.L: "Effect of Gaseous Fluids on Submersible Pump Performance,'' paper SPE 9218 published in the *JPT* (December 1982) pp 2922-2930
3. Pessoa, R., Machado, M., Robles, J., Escalante, S. and Henry, J.: "Tapered Pump Experimental Tests with Light and Heavy Oil in PDVSA INTEVEP Field Laboratory," SPE-ESP Workshop (April 1999).
4. Pessoa, R " Experimental Investigation of Two-Phase Flow Performance Of Electrical Submersible Pump Stages," MS Thesis, The University of Tulsa (2000).
5. Romero, M.: *An Evaluation of an Electric Submersible Pumping System for High GOR Wells,* MS Thesis, The University of Tulsa, Tulsa, Oklahoma (1999).
6. Sachdeva, R.: *Two-Phase Flow Through Electric Submersible Pumps,* MS Thesis, The University of Tulsa, Oklahoma (November 1998).
7. Sachdeva, R., Doty, D.R., and Schmidt, Z.: "Performance of Axial Electric Submersible Pumps in Gassy Well", paper SPE 24328 presented at the SPE Rocky Mountain Regional Meeting held in Casper, Wyoming. (May 18-21, 1992).
8. Turpin, J.L., Lea, J.F. and Bearden, J.L.: "Gas-Liquid Flow Through Centrifugal Pumps-Correlation of Data," 3rd Int'l Pump Symposium, Texas A&M University (May 1986).
9. Sun, D., Pessoa, R. and Prado, M.: "Single-Phase Model for Radial ESP's Performance" TUALP ABM. Tulsa, OK November 17,2000.
10. Pessoa, R, Sun, D. and Prado, M.: "State of the Art: Experimental Work on ESP Performance under Two-Phase Flow Conditions", TUALP ABM. Tulsa, OK November 17,2000
11. API Practice for Electrical Submersible Pump Testing," second edition , august 1997
12. Kallas, P and Way K ,:" an electrical submersible pumping system for high GOR wells," SPE Electrical submersible pump workshop, April 26-28, 1995
13. Wilson, B.L .: " Gas handling centrifugal Pumps," SPE electrical submersible pump Workshop, (1998)

ACKNOWLEDGEMENTS

The authors appreciate the technical and financial support of Tulsa University Artificial Lift Projects' member companies. The progress on this work is the result of the support of ENI - AGIP, CENTRILIFT, PDVSA, PEMEX, ONGC, SCHLUMBERGER, SHELL and TOTALFINA ELF.

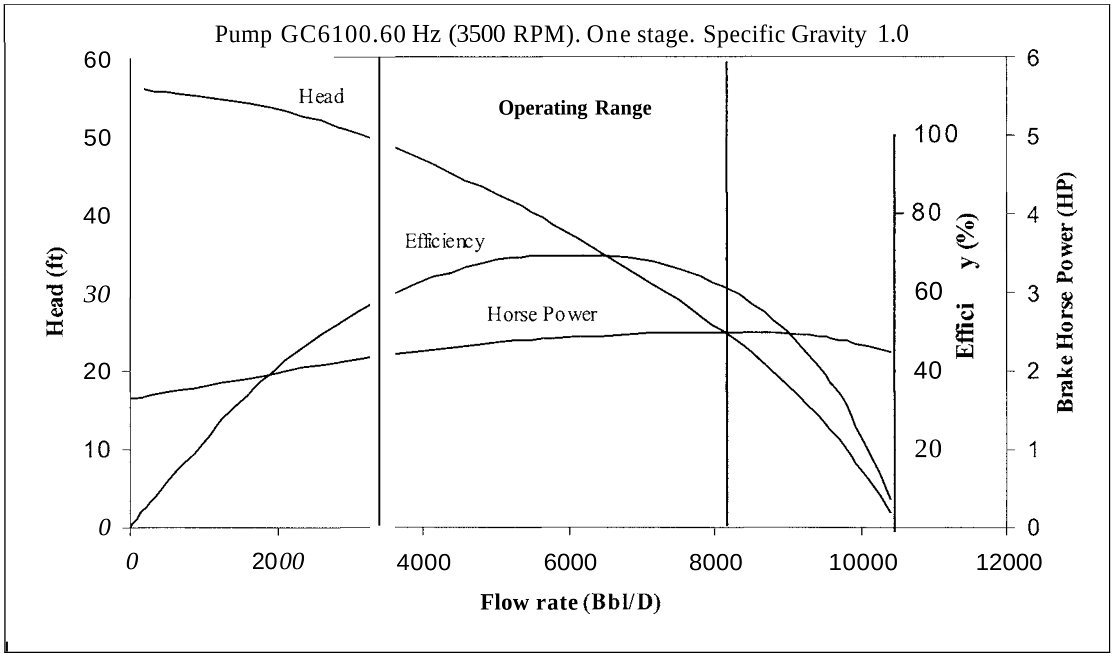

Figure 1 - Manufacturer Pump Performance Curves

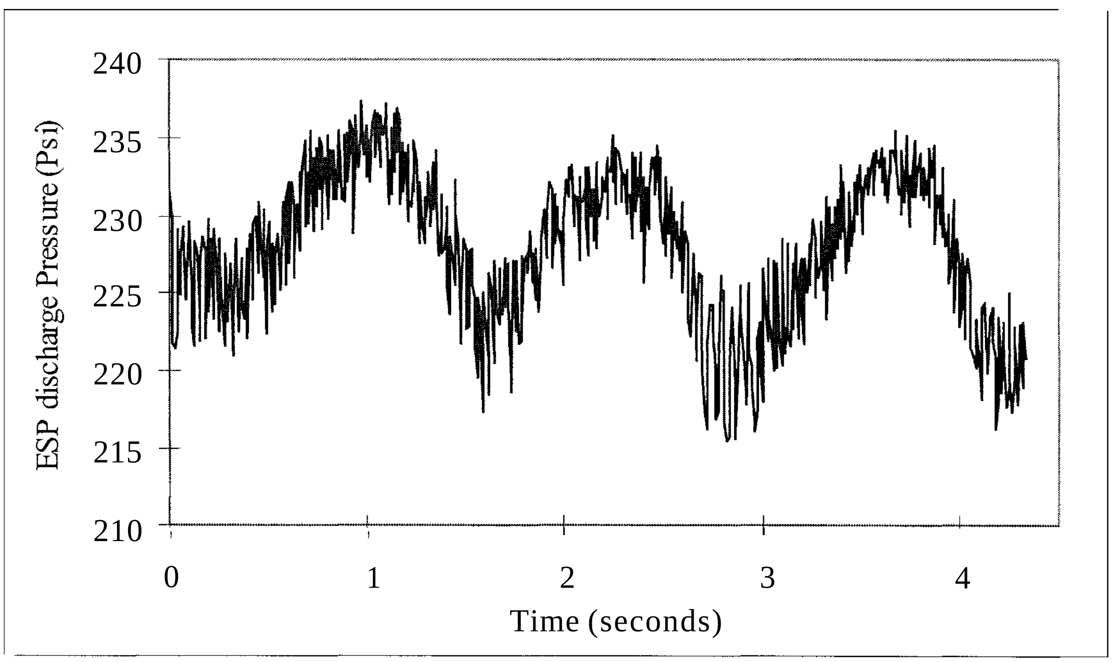

Figure 2 - Pump Discharge Pressure Fluctuation During Surging Condition

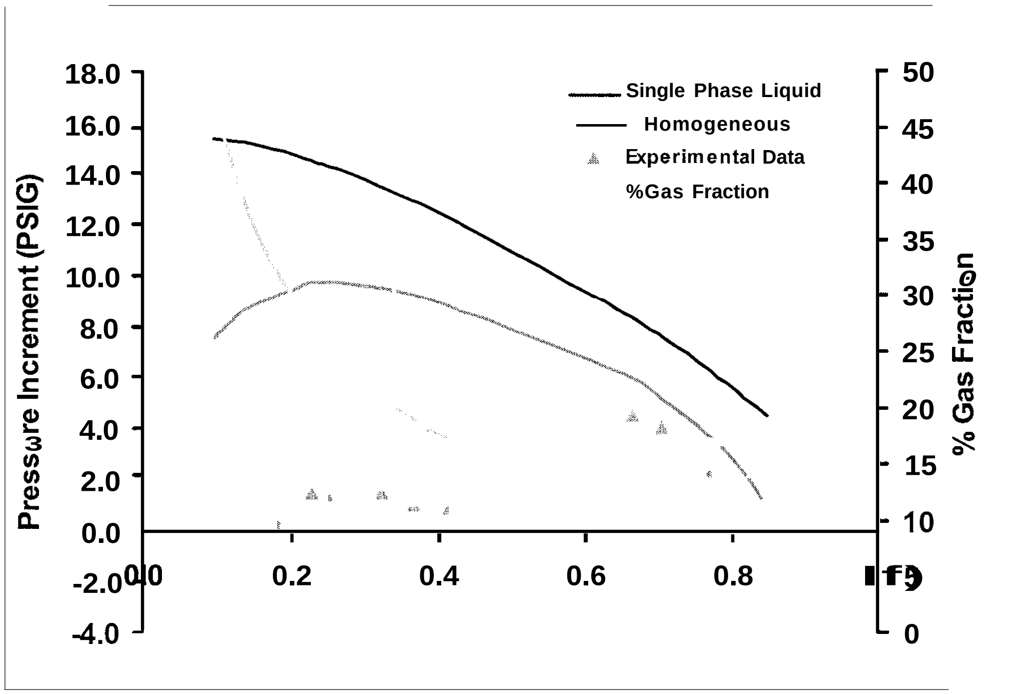

Figure 3 - Comparison of Pump Average Performance with Single-Phase and Homogenous Model

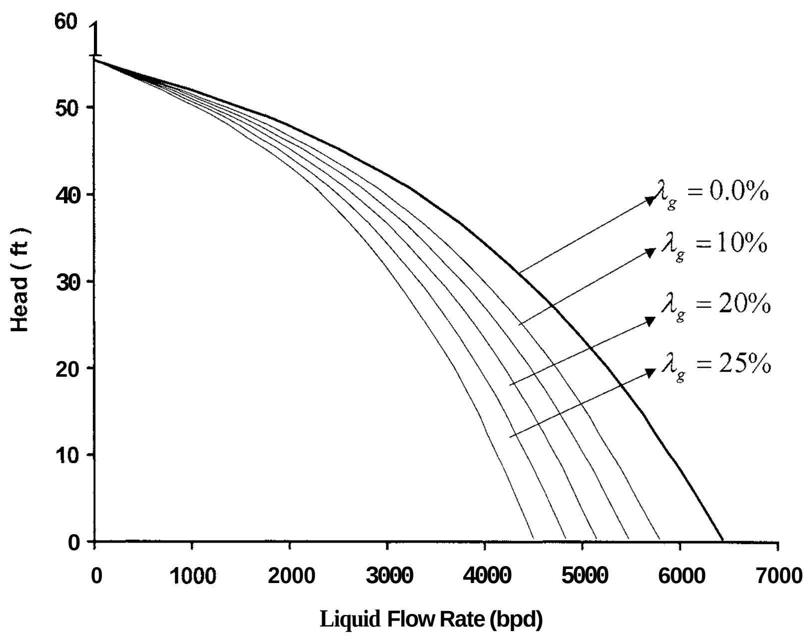

Figure 4 - Development of Homogenous Model

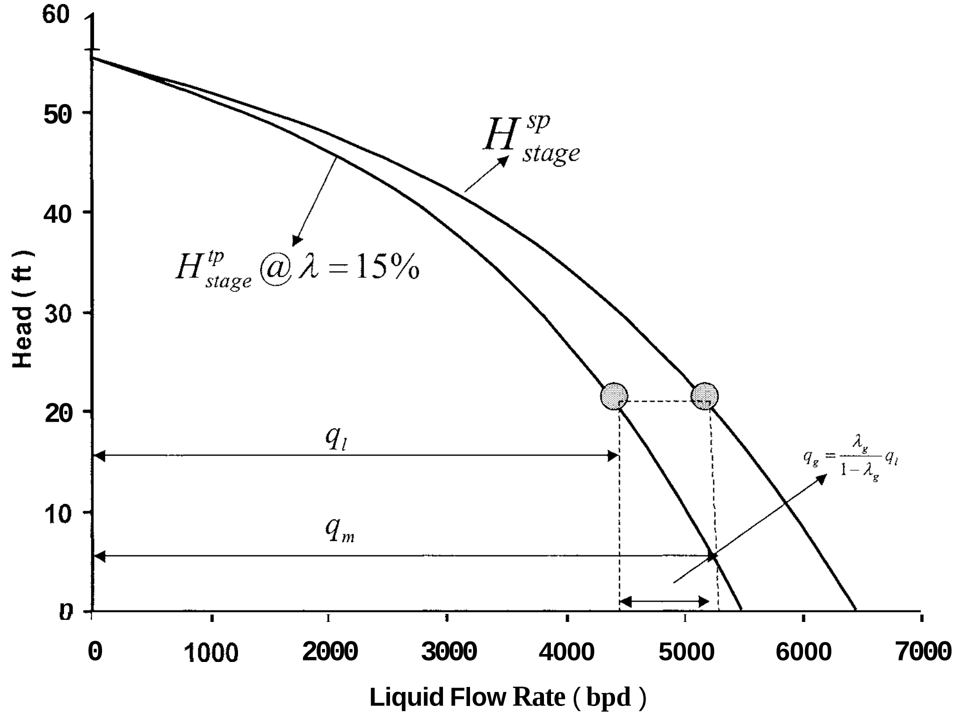

Figure 5 - Homogeneous Model for Different Gas Void Fractions

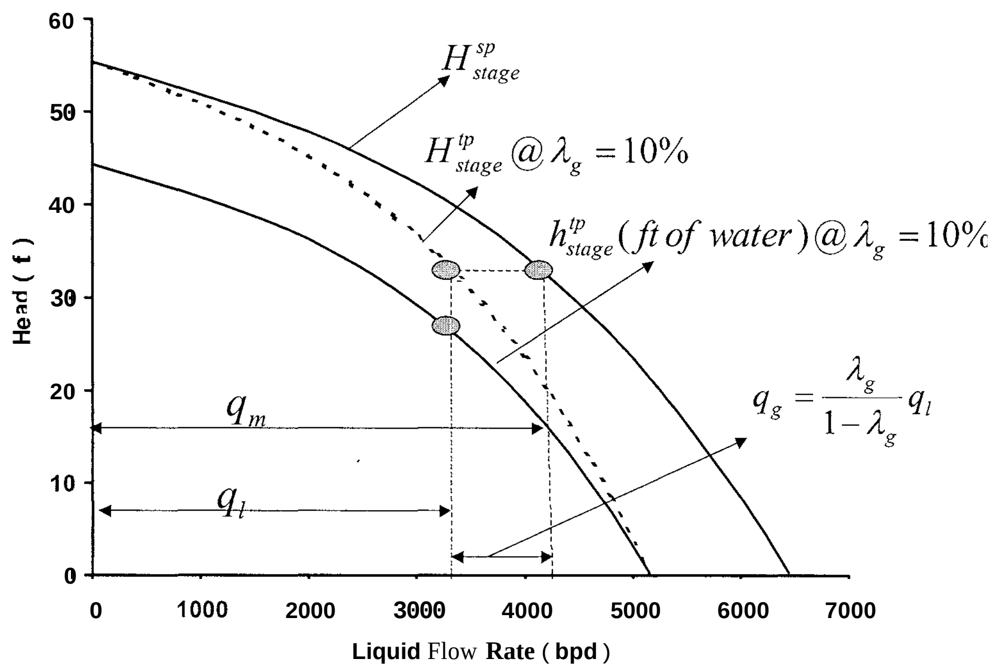

Figure 6 - Homogeneous Model Based on Water Density

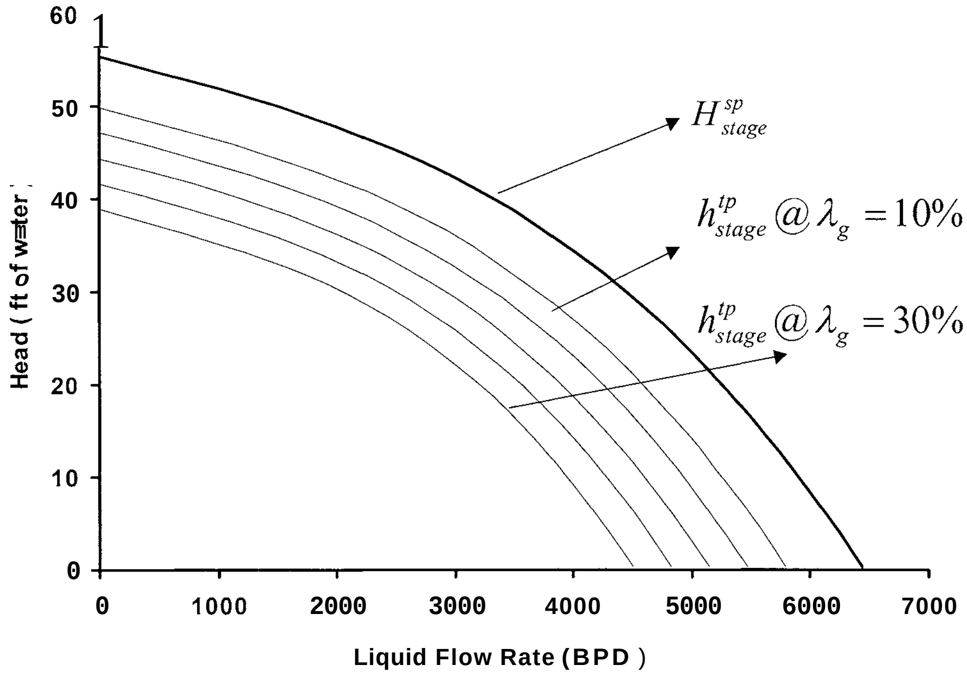

Figure 7 - Homogeneous Model for Different Gas Fractions Based on Water Density

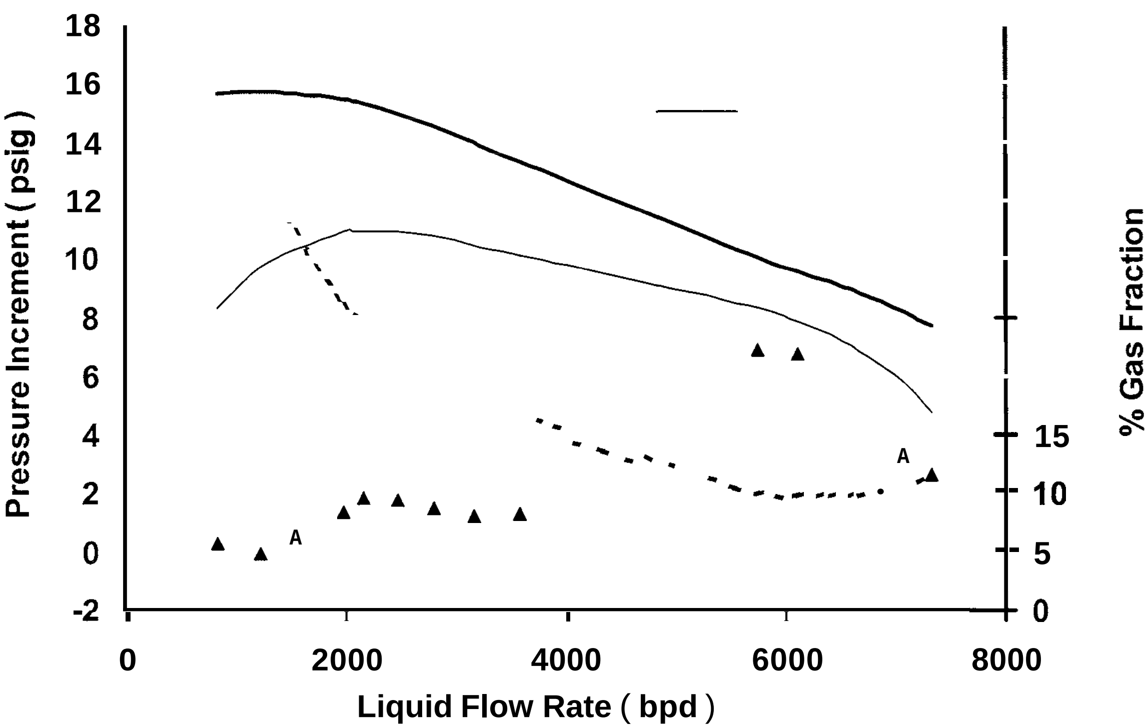

Figure 8 - Comparison of Homogeneous Model with Experimental Data

Figure 9 - Dunbar Curve

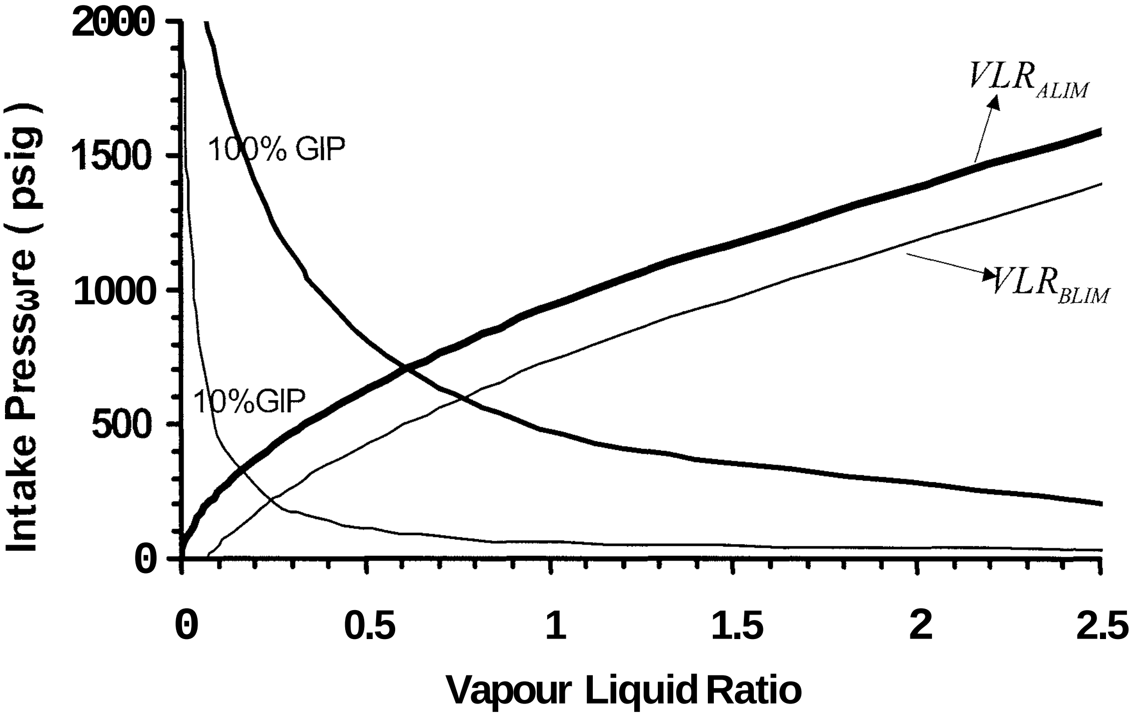

Figure 10 - Dunbar Curve Super Imposed with Gas Ingestion Percentage Curves

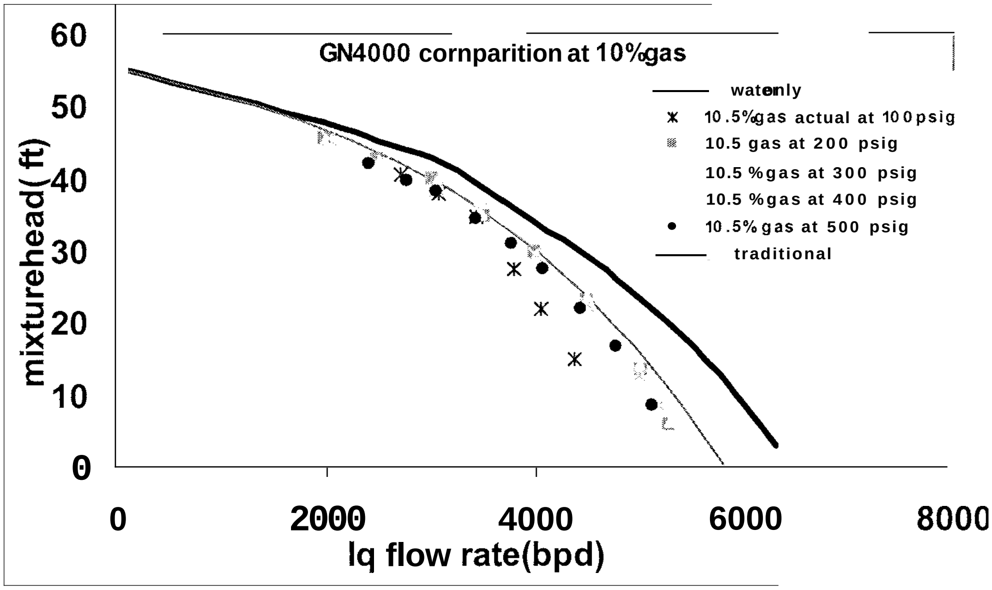

Figure 11 - Comparison with Homogeneous Model

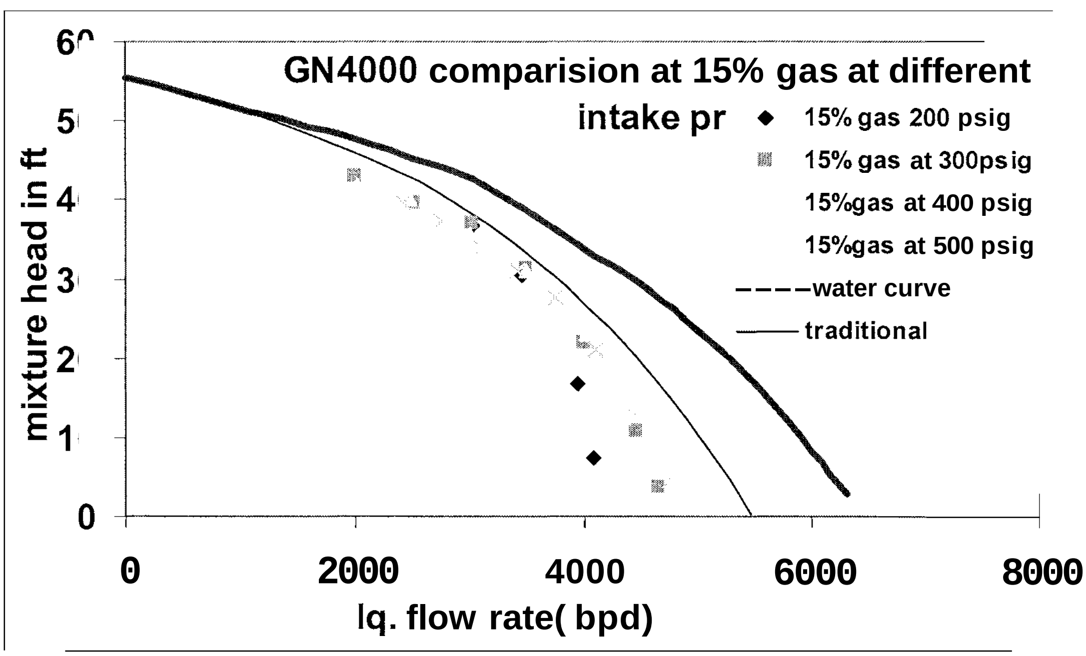

Figure 12 - Comparison with Homogeneous Model

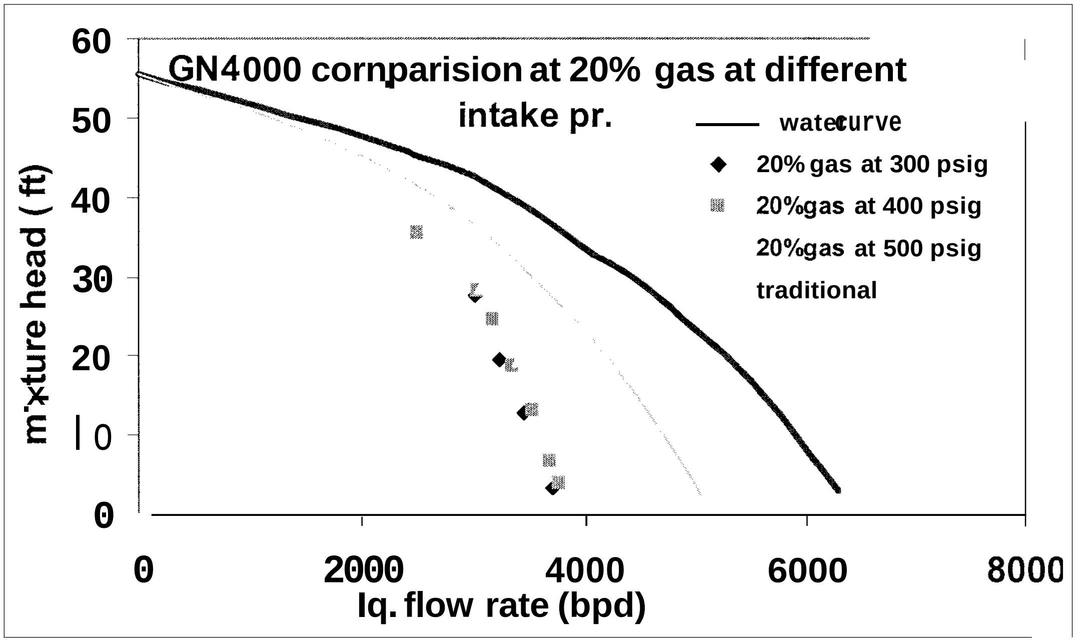

Figure 13 - Comparison with Homogeneous Model

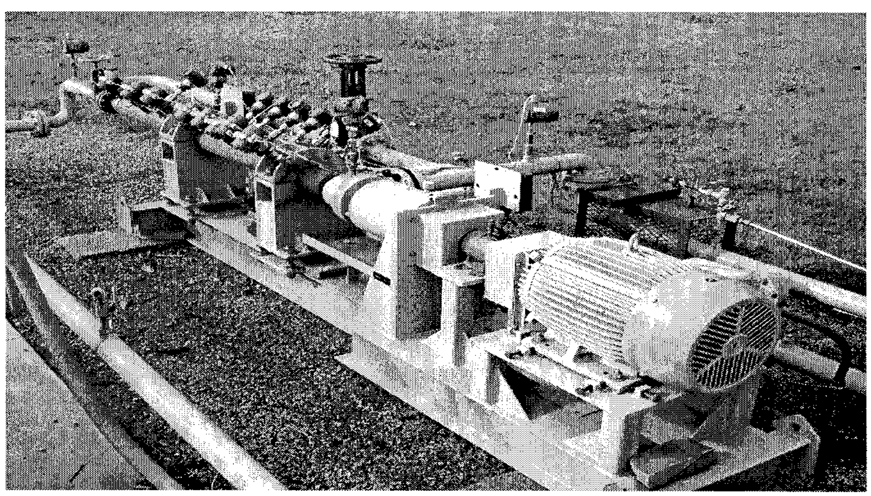

Figure 14 - ESP Test Bench After Modifications

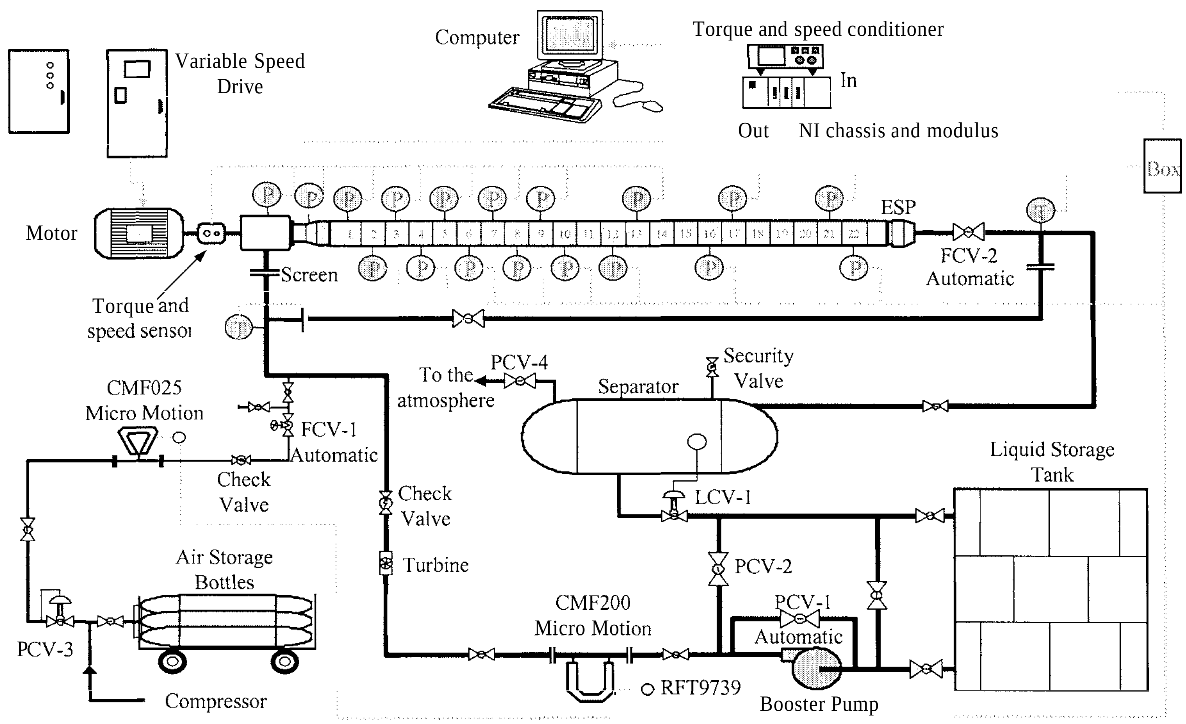

Figure 15 - Facilities Setup

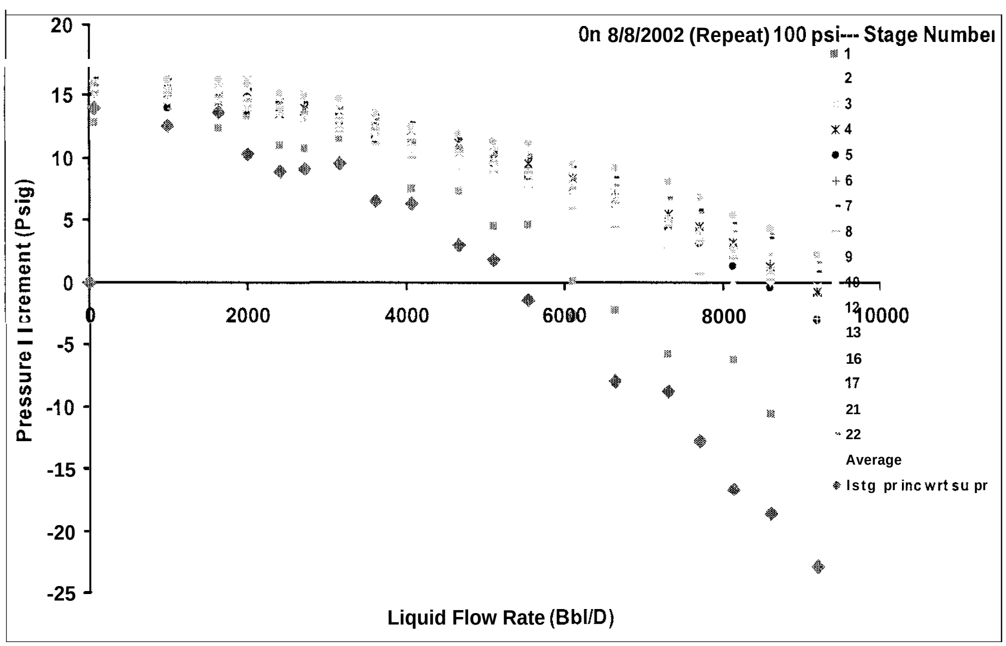

Figure 16 - Single Phase Performance at 100 Psi

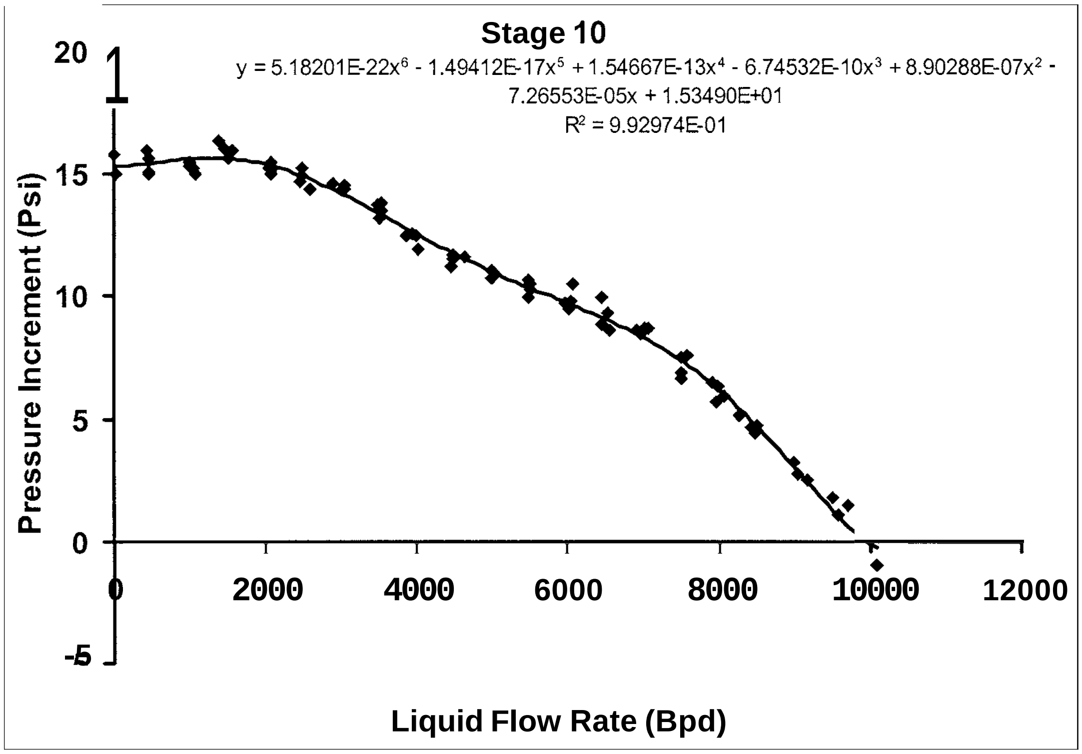

Figure 17 - The Average Performance of 10 Stages Pseudo Pump

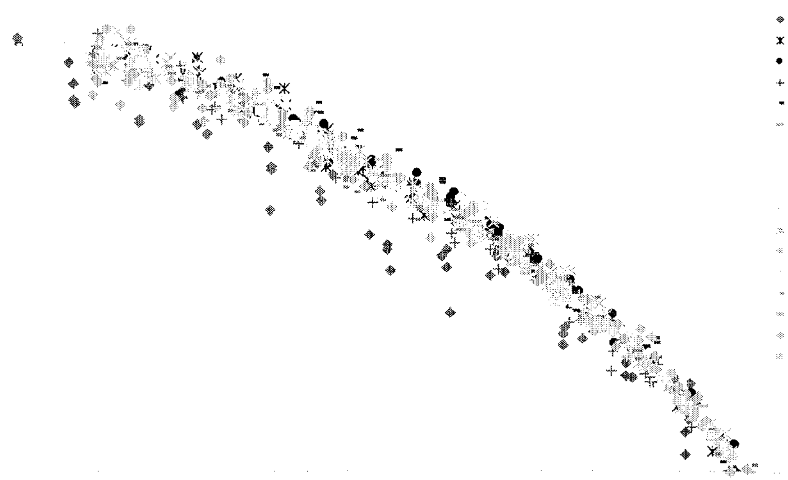

Figure 18 - Stage-wise Dimensionless Performance

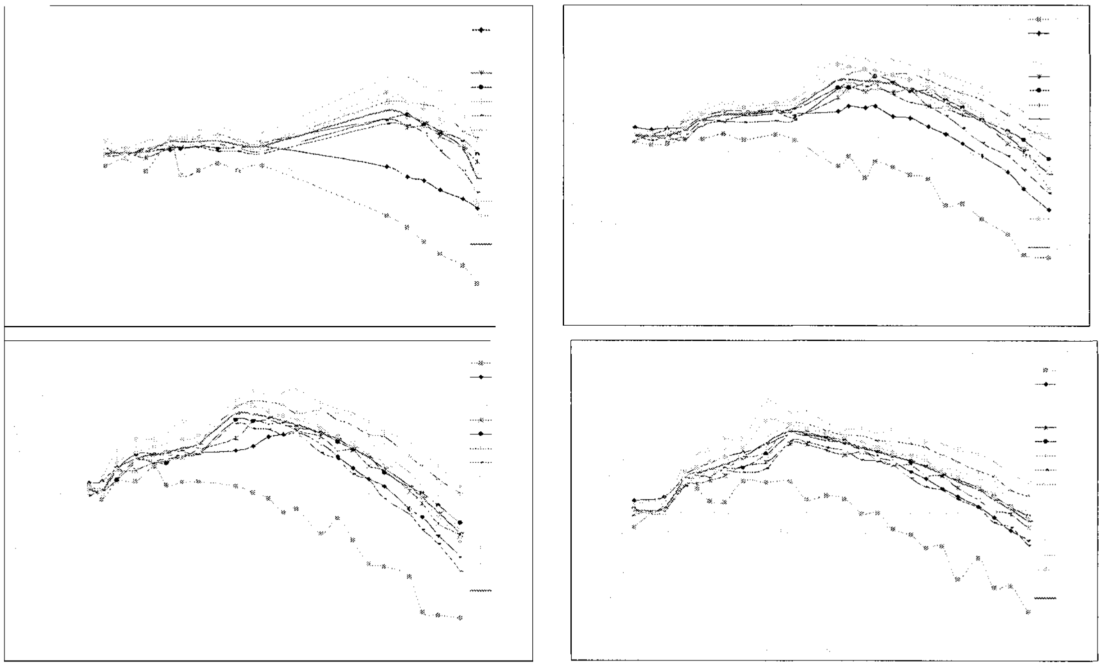

Figure 19 - Stage-wise Performance at Different Intake Pressure for a Gas Flow Rate of 30000 scfd

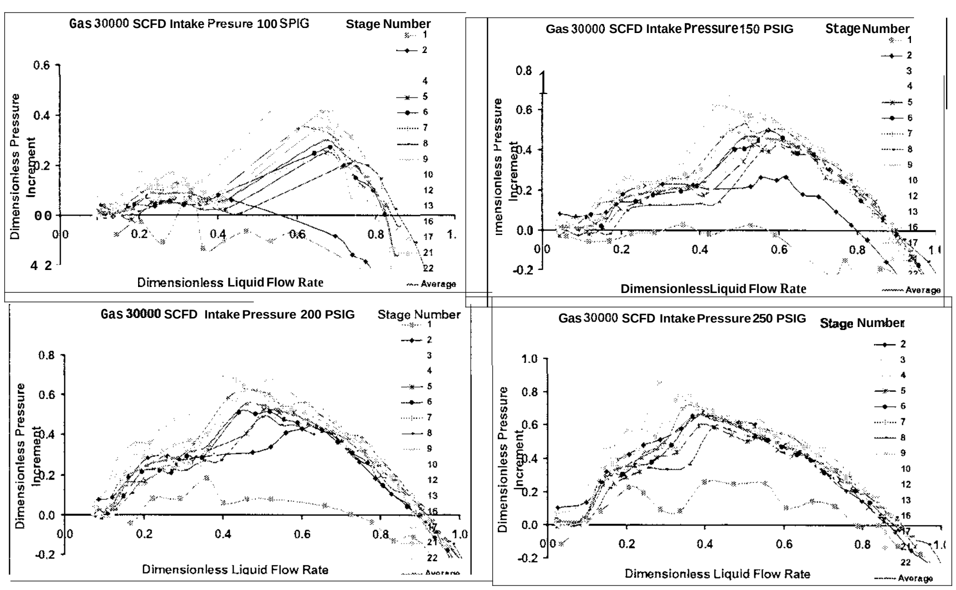

Figure 20 - Dimensionless Performance of Stages at Different Intake Pressures for a Gas Flow Rate of 30000 scfd

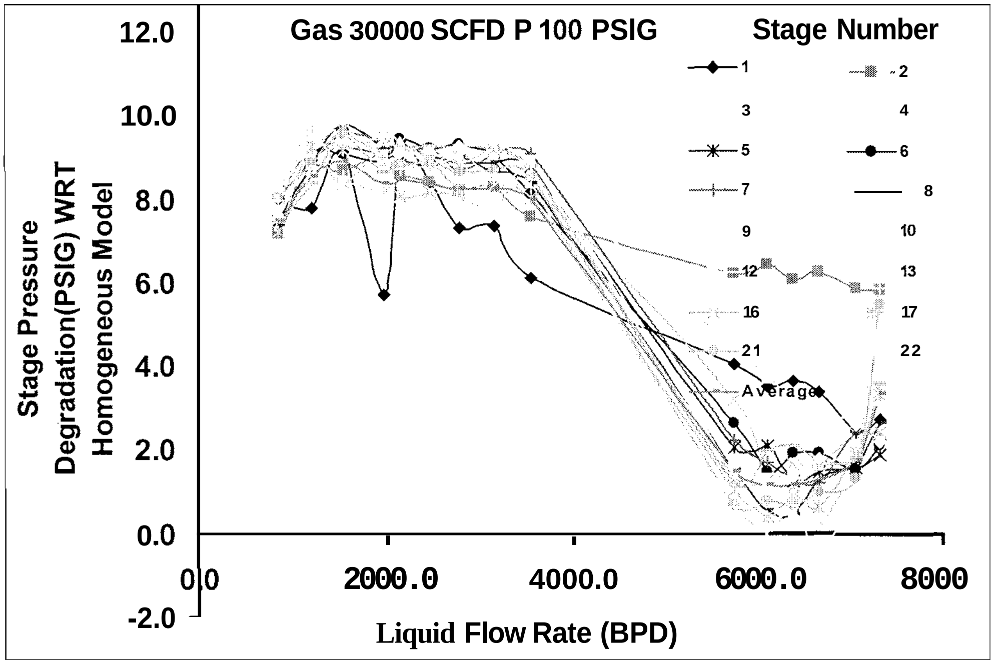

Figure 21 - Stage-wise Performance Degradation wrt Single-Phase at Gas 30000 SCFD-Pressure 100 psig

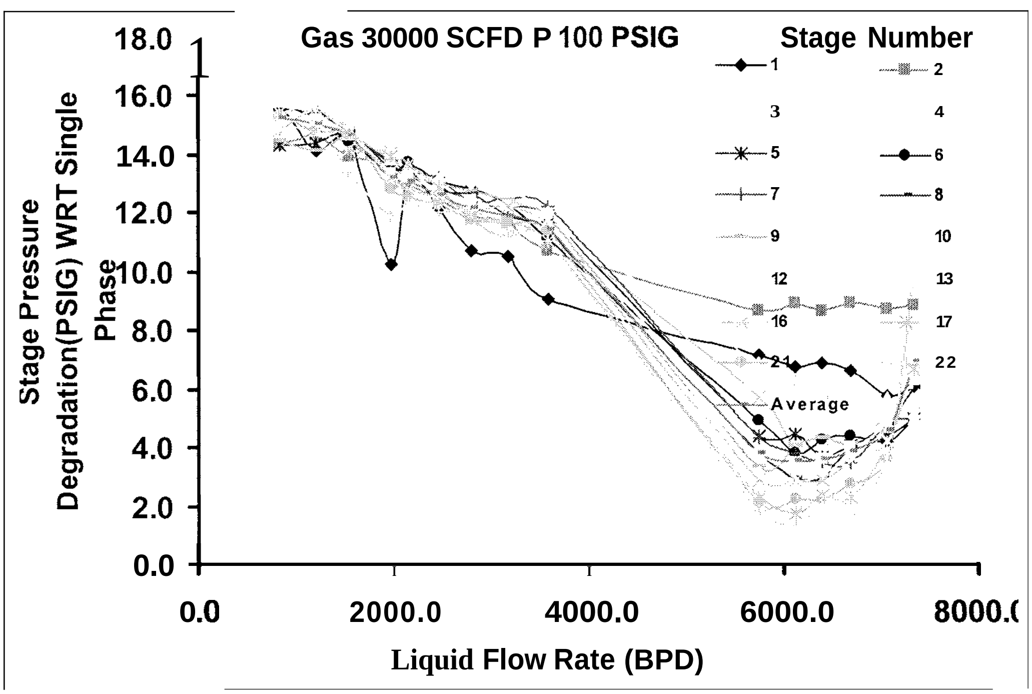

Figure 22 - Stage-wise Performance Degradation wrt Homogeneous Model at Gas 30000 scfd-Pressure 100 psig

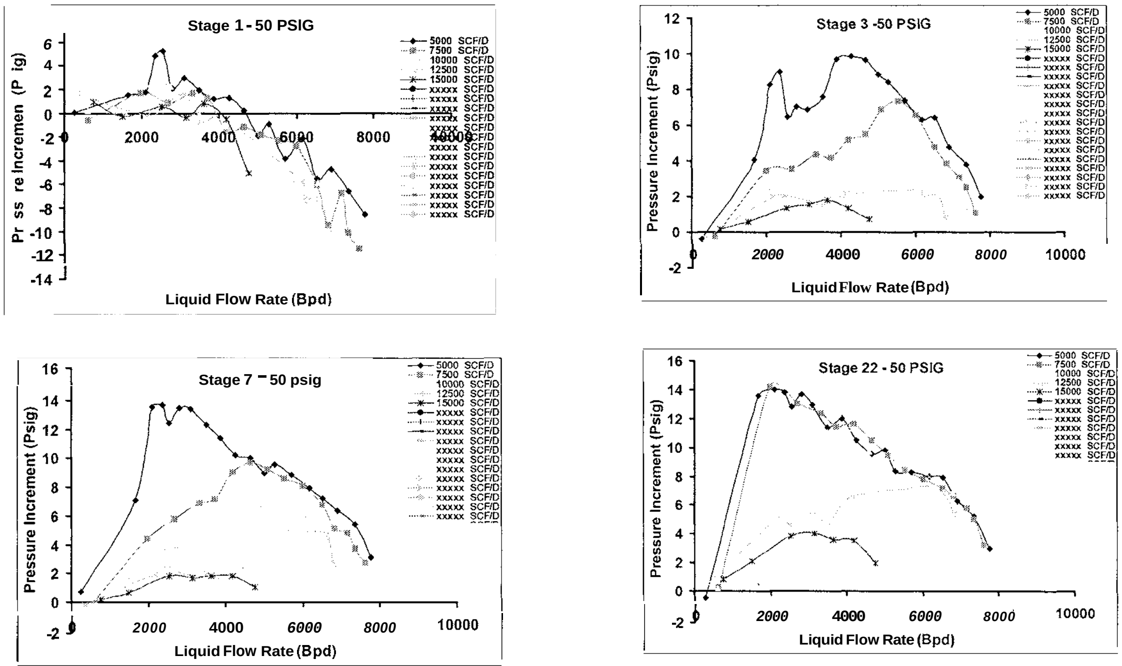

Figure 23 - Example Showing Effect of Stage Position

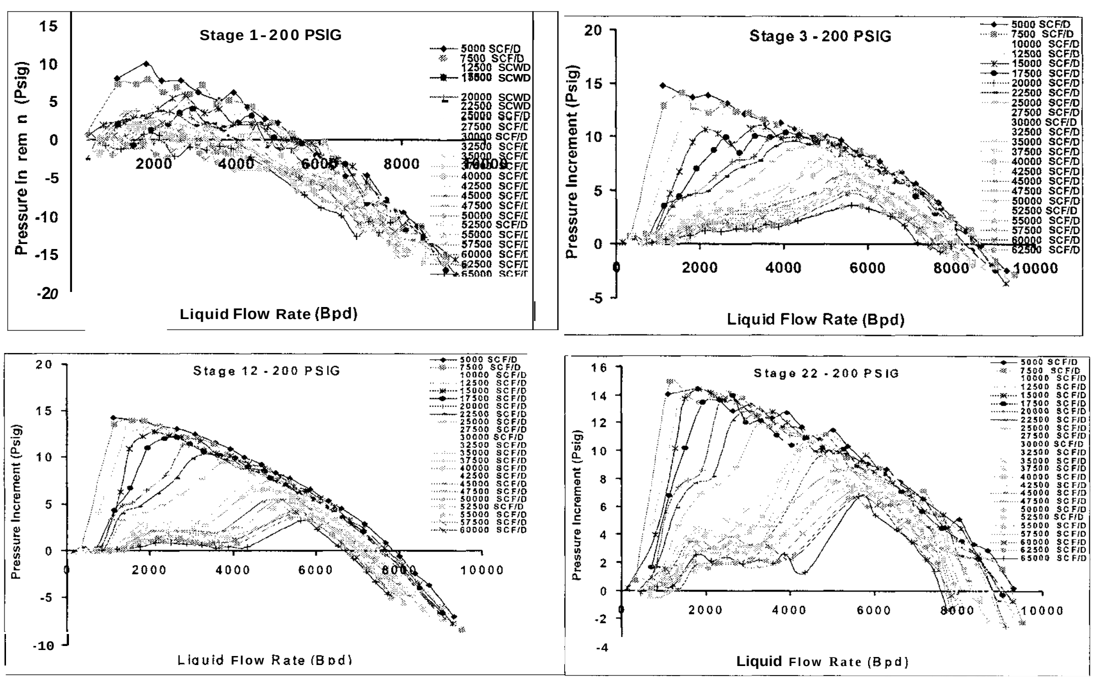

Figure 24 - Effect of Stage Position at the Intake Pressure of 200 psig

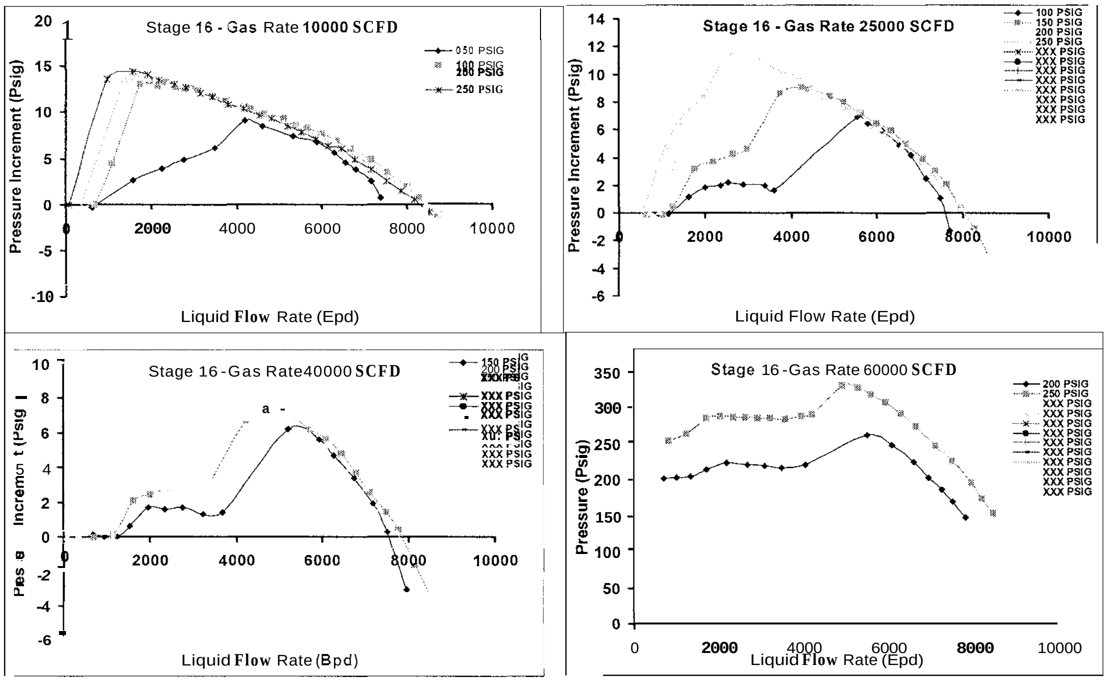

Figure 25 - Example for Effect of Pump Intake Pressure on Stage Performance

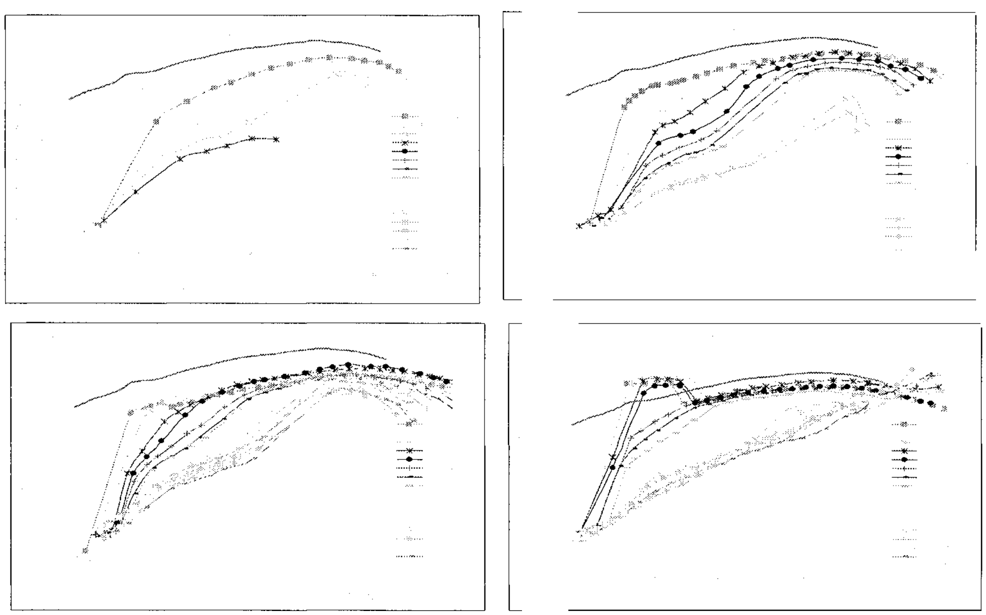

Figure 26 - Plot Showing Average BHP Consumption at Different Intake Pressure

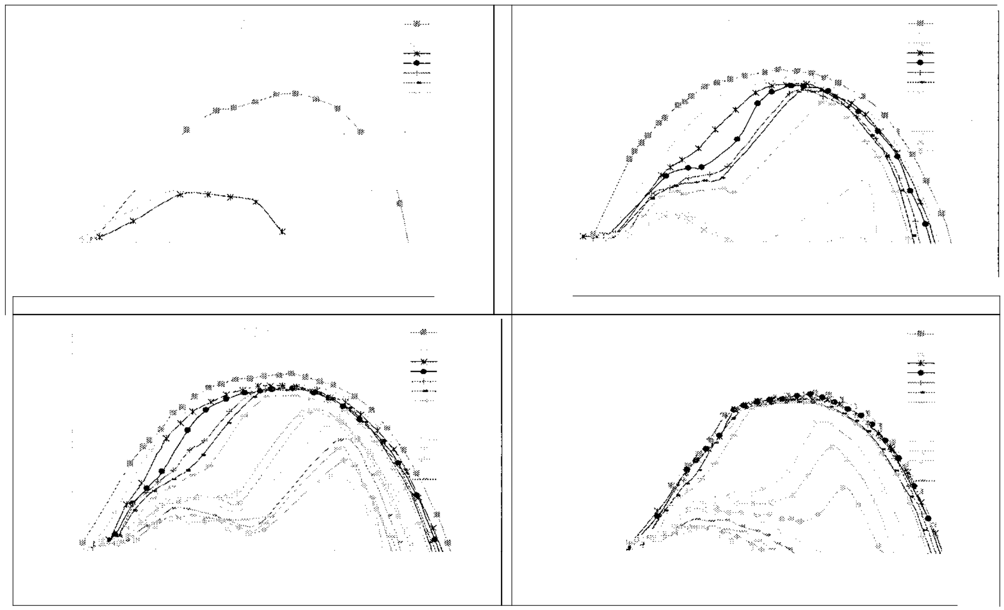

Figure 27 - Efficiency Curves Based on Adiabatic Gas Compression